J Nanostruct 16(1): 444-453, Winter 2026

RESEARCH PAPER

NL-LIBS Between Nanomaterial and Bio-Sample

Noor Malik Saadoon [1], *Ahmed J. Jasim* [2]

[1] *Centre of Nanotechnology and Advanced Material, University of Technology, Iraq*

[2] *College of Medical Engineering, University of Technology, Iraq*

ARTICLE INFO

Article History:
Received 15 August 2025
Accepted 06 December 2025
Published 01 January 2026

Keywords:
LIBS
Bio-samples
Carbon lines emission spectrum
MgO NPs

ABSTRACT

Laser induced breakdown spectroscopy is potent tool used to explain the interaction of laser with the material of all type and variety fom bulk material to Nano mater and bacteria by analyzing the consequent plasma emission of the specimen by analysis its emission spectrum. In these works we focused on synthesis of nanomaterial and studied the effect of MgO-NPS as an anti - bacterial agent. later we diagnosed the emission spectrum generated by the interaction of laser and the particular bacteria were Staphylococcus aureus and Escherichia coli. Software cycles called spectra-laser were used to scan libs spectra. The spectra of the glass substrate LIBS as well as those of the microorganisms were compared. There was Fe, Magnesium, Na, K, Ca P, S, calcium, and aluminum, Manganese, Copper Carbon, Hydrogen and CN-band in bacterial samples. Escherichia coli and Staphylococcus aureus revealed two lines of carbon 193.02 nm and 247.88 nm and a single H line with ratio of 656.28 nm1.53 and 1.9, 1.83uratively to the amount ratio of 656.28 nm Carbon and hydrogen are the most important components that bacteria and other cancer cells that constitute the bio-samples are composed of. The findings indicated the importance of LIBS in identification and differentiating between different types of bacteria.

How to cite this article
Saadoon N, Jasim A . NL-LIBS Between Nanomaterial and Bio-Sample. J Nanostruct, 2026; 16(1):444-453. DOI: 10.22052/JNS.2026.01.040

INTRODUCTION

Laser-induced breakdown spectroscopy (LIBS) is a commonly observed type of spectroscopic analysis that employs intense beam of laser light, which was being focused on the surfaces of the target, and vaporize, excite, and ionize on the target species. When an excited state is de-excited (or atoms are recombined) light is produced and the light is gathered and spectrally analyzed to extract beneficial information, most notably the identification of elements, the magnitude of elements and the calculation of the electron temperature and the electron number density of the plasma. The baseline characteristics and dynamics of the plasma are contingent upon a wide range of laser parameters, including wavelength, pulse duration, power density and the nature and composition of target material [1 3]. LAS (Laser Ablation Spectroscopy), and LSS. In these methods, the radiation of the plasma is laser (determining spectrum after focusing it on the sample). Target substantial is open-weather in height pulsed laser beam (normally >1-10, MW/cm2) in spectrochemical video when employing the LIBS technology. After the dissolution, the sample will result into the transient formation of energetic

* *Corresponding Author Email: mae.visit.04@uotechnology.edu.iq*

quantities of plasma. Each pulse causes de-excitation of the atoms and the fusion of electrons due to plasma cooling. After only a small amount of plasma continuous emission remains, LIBS spectra appear. The crucial details of this spectroscopic method have been addressed in several studies [4-5]. Due to numerous advantages, LIBS technique can apply widely to any field but forensics, public health, environment and pharmaceutical [6-10]. The method has been previously utilized many times to investigate aspects within many biological systems. These studies examine a target sample and rapidly determine the organic and inorganic elemental composition with a high persistence (typically >1-10 MW/cm2). A simple analysis of several biological systems occurs when the sample separates. These analyses make it possible to rapidly perform high-resolution identification of the organic and inorganic elemental composition [11–19]. Several studies have been reported, which deal with identification, classification and recognition of bacterial samples using LIP [20-25], the complex and multifaceted nature of which is more engaging than carbon-based and biological materials. Baudelet et al examined spectra of two types of bacteria, Bacillus subtilis and Escherichia coli and wrote down their spectra that contacted lines at a separation of 13 atomic or molecular species. Rehse group [26,27] has applied LIBS to analyze microorganisms of Pseudomonas aeruginosa. In the emission spectra, the researchers have noticed 19 sub microscopic and ionic lines to identify and classify the bacteria. Our work will offer comprehensive LIBS scrips on the varied bacterial strains such as Micrococcus luteus, Staphylococcus aureus and Escherichia coli as well as nano-material MgO.

MATERIALS AND METHODS

Nanomaterial Synthesis MgO

The aqueous solution of Magnesium Nitrate hydroxide has been prepared as follows. 0.02 moles of Magnesium Nitrate hydrate, Mg $(NO_3)_2.6H_2O$ was dissolved in 100 ml of the distilled water to get the aqueous solution of Magnesium Nitrate hydroxide. Magnesium Nitrate hydrate combinations and distilled water were stirred during 4 hours to clarity. A stirring, ammonia has been added drop-by-drop to Magnesium Nitrate hydrate solution to adjust to pH equal to 9. A precipitate was immediately obtained by washing the precipitate obtained and carefully washed repeatedly using methanol and distilled water to which was filtered and then dried overnight in the oven at 100°C. Samples were then ground and annealed in Muffle furnace at 500°C temperature within three hours. Finally, the white Nano powder was obtained. The powder obtained was re-grounded and the addition of the ad mixture made and less than 15 tons passed through using 1.5 cm diameter target compressor. The obtained target was as dense and homogenous as possible in order that the quality of the deposit was good.

Sample accumulating

the strains of bacteria used in this study were Gram-negative and Gram-positive and micrococcus luteus which were supplied by the contamination research center/ ministry of science and technology (Baghdad, Iraq). Staphylococcus aureus, E. coli and Micrococcus luteus were all cultured in nutrient agar plates at 37 °C. One colony was picked in a sterile loop and inoculated in 10 mL nutritional both and held overnight at 37 °C. After they were completed, the S. aureus and E. coli at 108 cfu/mL, 106 cfu/mL, 104 cfu/mL, 103 cfu/mL, 100 cfu/mL, and 10 cfu/mL in each medium were centrifuged at 6000 rpm during 5 min. To avoid the presence of medium and debris, the cells were centrifuged three times and later repeated after deferring a second time in 500 1 of phosphate-buffered saline (PBS). All supernatants were discarded. Once all the supernatant had been removed after the final wash, cells were transferred into PBS through pipetting to ensure uniform spreading prior to their addition to the well.

LIP System

In the experimental set-up, Nd: YAG laser as the source of illumination frequency at a wavelength of 1064nm and used 850milli joules per pulse repetition frequency of 10Hz pulse width 6ng laser pulse energy meter was connected to receive the laser energy measurements onto the flash lamp Q-switch delay which were run via laser controller. Spectrometer (Nova-Quantel P/ niz01507) Spectrometer (Ocean Optics Inc. HR 4000) The spectrometer possesses 14 gratings whose appearance slits can be 5, 10, 25, 100, or 200 nm. It ranges over 2001100nm, with an optical measurement of 0.03nm (FWHM) and an integration time of 3.8ms[10] Secondary Spectral Lines were determined using the assistance of

LIBS Analyzer program that in order to catalogue and characterize the bacteria has the necessary lines of the (NIST) In this case, we demonstrate a professional LIBS analysis of 3 bacterial types, S. Staphylococcus aureus and Escherichia coli and MgO NPs spectra.

RESULTS AND DISCUSSION

Characterization of MgO materials

The powder XRD method was used to identify the crystal phase of MgO nanoparticles with Philips diffractometer of the X-ray as the source of Cuka radiation with wave length of 0.15406 nm. It has been identified by Fig. 2 that magnesium oxide exists at phase-cubic; no characteristic impurity peaks were observed. Typical reflection peaks at five MgO three were observed in Fig. 2 and indexed to the diffraction planes at (111), (200), (220), (3 1 1), and (222). a=b=c 4.130 is a cubic unit cell. Using highest peak (200), the Debye-Scherrer formula has been used and the average crystallite size has been calculated, $D=0.94\lambda/\Delta(2\theta)\cos\theta$. Where; D = average size of a crystallite, λ is the wavelength of the x-rays (1.504 nm), theta is Bragg angle of refraction and 26(2) is the FWHM which has been measured as a Gaussian curve at the Peak (200). Even the approximate value of the mean particle size of magnesium oxide could be assumed to be 55 nm [28].

Scanning Electron Microscopy (SEM)

SEM images of the synthesized nanomaterial are provided in Fig. 3. Here is accumulation of a many-layered aggregate particles. Man-made

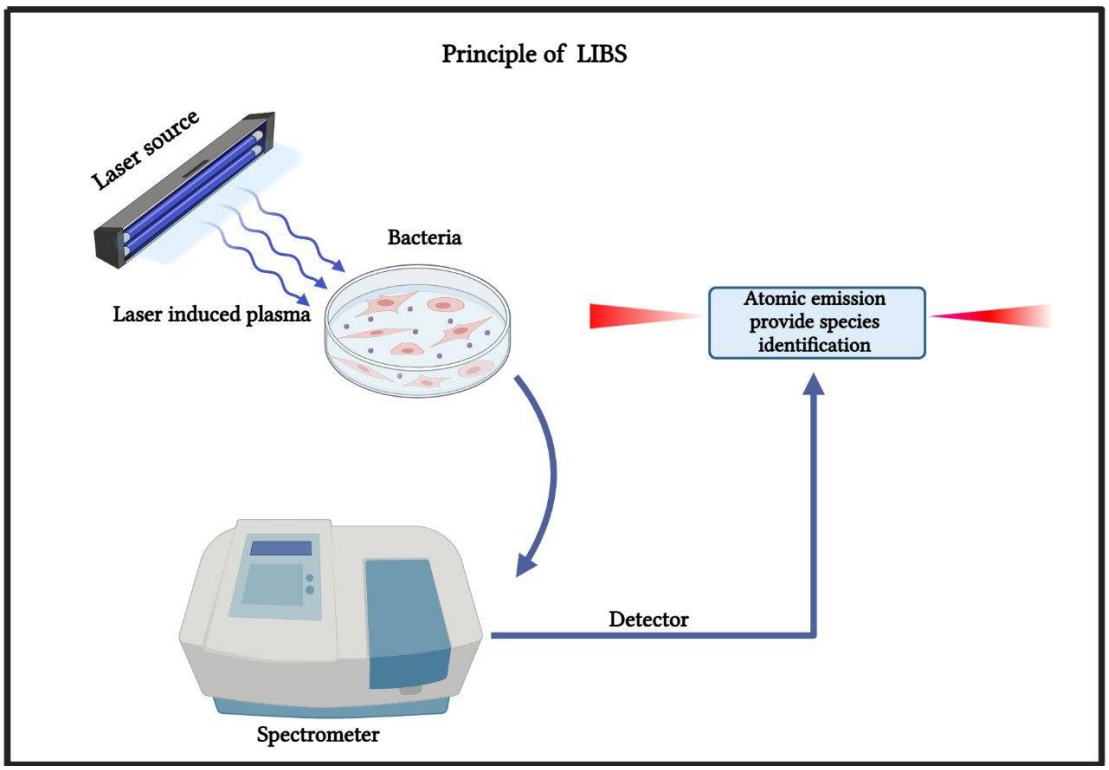

Fig 1: LIBS setup.

Table 1. Laser specification.

Parameters	Values
Beam diameter	7mm
Pulse width	6ns
Lased energy max	850mj
Repletion rate	10Hz

particles under nature are non-homogenous and crystalline [29].

Antibacterial activity

The antimicrobial activity of the X-SUBSTANCES so prepared was evaluated against Gram-negative (E. coli) and Gram-positive (S.aureus) bacteria employing the agar well diffusion method [30]. Sterile Petri dishes were aseptically filled with about 20mL of on MullerHinton (MH) agar. A sterile wire loop was used to collect a bacterial species of the stock cultures [31]. Once the organisms were cultured, 6 mm-diameter wells would be bored on the agar plates with of a sterile tip. The varying concentrations of the X-SUBSTANCES were put into the bored wells. The cultured plates

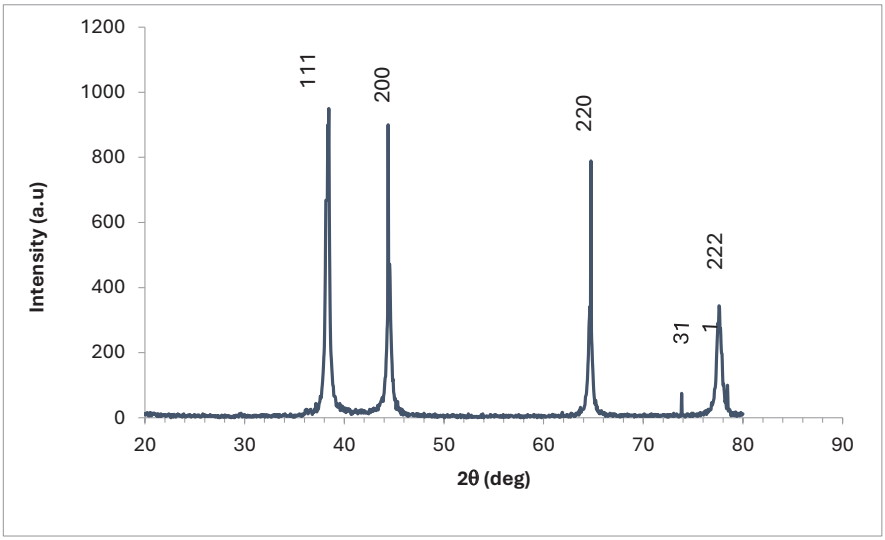

Fig 2. XRD pattern of MgO nanoparticle.

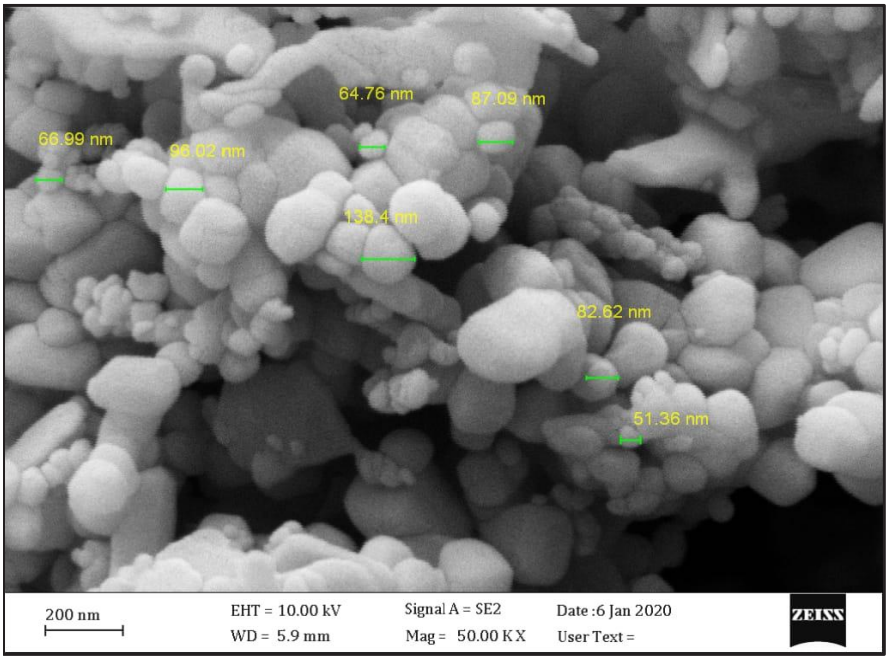

Fig 3. FE-SEM of MgO nanoparticles.

with X-SUBSTANCES and test organisms were left overnight at 37°C and the mean the zones of inhibition diameter [32] measured and recorded.

Statistical analysis

The data were analyzed statically with the help of Graphpad prism program Data are indicated as mean 6 SD of three experiments. Report significant difference statistically at p< 0.05 [33-36]. As illustrated in Figs. 4 and 5.

The emission spectra of magnesium plasma

The emission spectra of magnesium plasma Fig. 6 show the emission spectrum of magnesium plasma generated under the irradiation of 1064nm Nd: YAG laser. The figure represents the part of the emission spectrum which has closely separated multiple structure of neutral and small traces of singly ionized emission line of magnesium.The first structure is identified as 3s4s $^3S_1$ up to 3s3p $^3P_{0,1,2}$ transitions at 516.73nm, 517.30nm, and 518.50nm wavelength positions, and the second structure is identified as 3s5s $^3S_1$ up to 3s3p $^3P_{0,1,2}$ at 332.99nm, 333.21nm, and 333.66nm wavelength positions. The composite structure exists around 293nm is identified as 3s5s $^3S_1$ up to 3s3p $^3P_{0,1,2}$. There is another structure in Fig. 8, which corresponds to transitions 3s4d $^3D_{1,2,3}$ up to 3s3p $^3P_{0,1,2}$ at 309.14nm, 309.37, and 309.81nm, respectively. In addition, there are emission lines in the higher wavelength region among which the most dominant line at 880.68nm is identified as 3s3d $^1D_2$ up to 3s3p $^1P_1$ transition of magnesium. Two singly ionized magnesium transitions $2p^63p$ $^2P_{3/2}$ up to $2p^63d$ $^2D_{5/2}$ and 2p63s $^2S_{1/2}$ to $2p^63p$ $^2P_{1/2}$ three magnesium transitions, $3s3d^1D_2$ up to $3s3p^1P_1$ at 880.68nm,

3s5d $^1D_2$ → 3s3p 1P1 at 470.30nm, and 3s5s $^3S_1$ → 3s3p $^3P_1$ at 333.66nm have been selected.

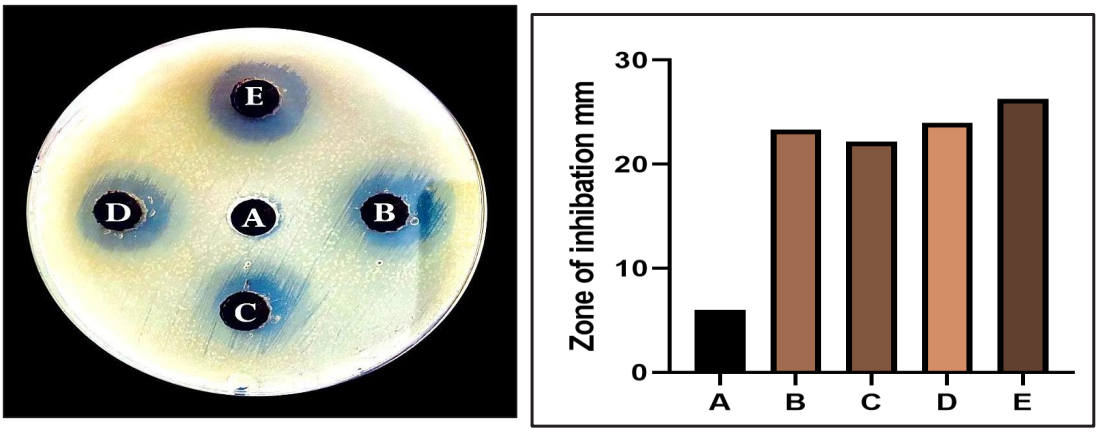

Fig. 4. Antibacterial activity of (N1) against *E.Coli.* A, control. B, 25%. C, 50%. D, 75%. E, 100%.

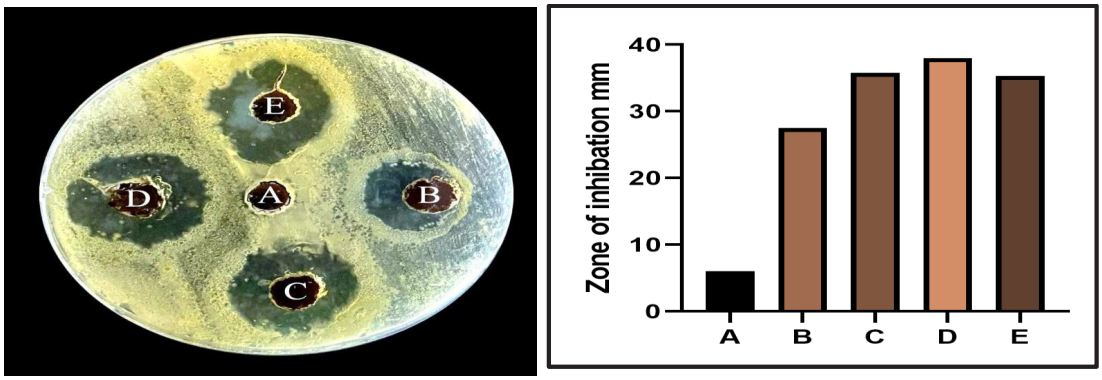

Fig. 5. Antibacterial activity of (N1) against *S.aureus.* A, control. B, 25%. C, 50%. D, 75%. E, 100%.

Bacterial cells emission spectra

The first to measure the arrangement of protoplasm in connection with those materials of attachment that are laid down in the form of lipids and poly-saccharides was Gunsalus and Stanierin (1960) they. X-ray microanalysis was used to quantify carbon, phosphorus, O2, N 2 and S in various cells of natural aquatic samples and cultured bacteria sample. E. coli, S. aureus, and Micrococcus luteus bacterial plasma spectroscopy emission are presented in Figs. 9, 10 and 11 respectively. [3536]. The researchers employed LIBS in air to detect the emission of the major and minor bacterial cell contained trace amounts of manganese, copper and aluminum together with the elements of sodium, potassium, Ca, Mg

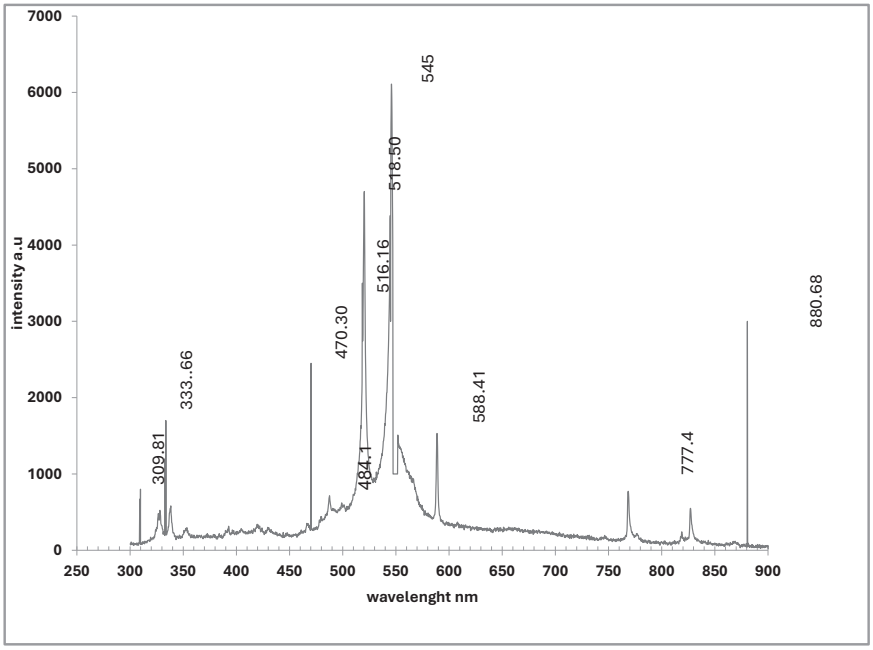

Fig. 6. Portion of the emission spectrum of magnesium produced using 1064nm laser wavelength.

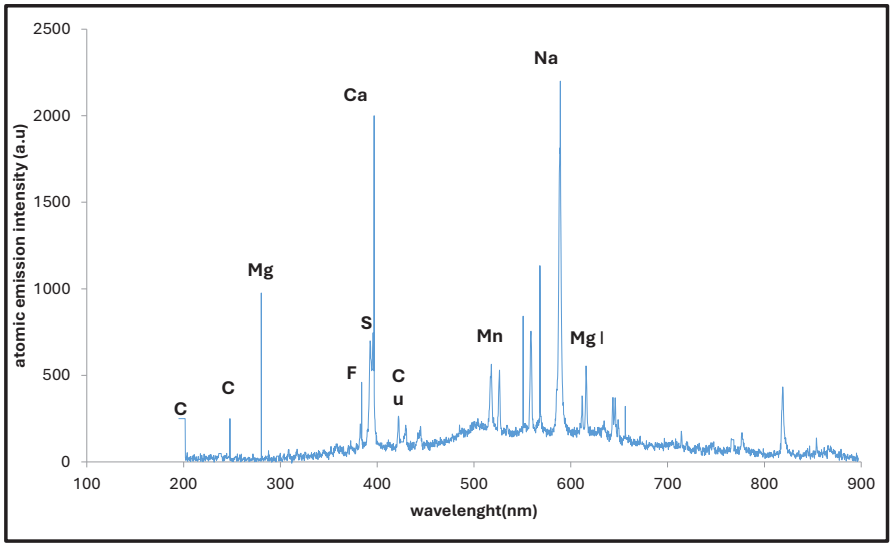

Fig .7.LIBS spectrum of bacteria E.Coli.

phosphorus, sulfur, chlorine and Fe. To ensure a clean surface on each shot, the investigational data was collected at ten shot is more or less on a rotated sample. Plasma spectra of bacteria, E. Coli, S. aureus and Micrococcus luteus have been illustrated in Figs. 7, 8 and 9 respectively. We

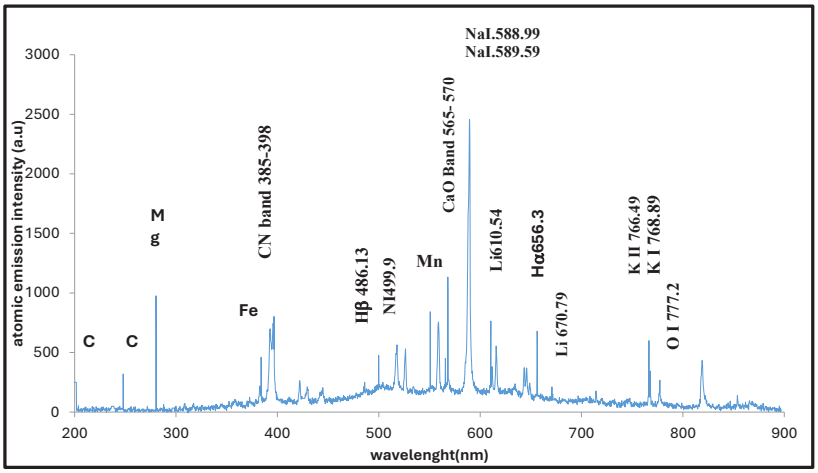

Fig .8.LIBS spectrum of acteria S. aureus.

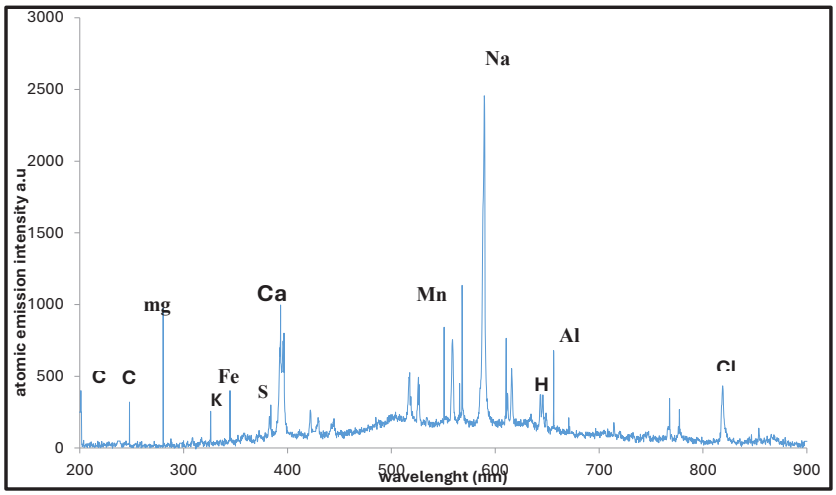

Fig 9. Emission of bacteria *Micrococcus luteus.*

Table 2. Components distinguished in bacterial spectra.

No	Element	Wavelength (nm)	Lower level conf, term	Upper level conf term
1	Ca	396.84	$3P^6 4s^2 S$	$3P^6 4P^2 P^0$
2	Mg	280.27	$2s2p^3(^3D^0)3d^4p^0$	$2s^2sp^2(^3P)\ 5s^4P$
3	Na	568.26	$2p^6 3p\ ^2P^0$	$2P^6 4d\ ^2D$
4	K	344	$3p^6 4s\ ^2S$	$3p^6 6p^2 P^0$
5	P	856,875,415.033	-	-
6	S	393.32	-	-
7	Cl	837.596	$3S^2 3P^4(3P)4s\ ^4P$	$3S^2\ 3P^4\ (3P^0)\ X\ ^1G^0$
8	Fe	383.92	$3d^7(^2G)4sa\ ^1G$	$3d^6(^3F2)4s4p(^3p^0)x\ ^1G^0$
9	Al	662.884	$3s4d\ ^1D$	$3s7p\ ^1p^0$
10	Mn	550.587	$3d^5 4s^2 a\ ^4G$	$3d^6(^5D)4pz^6F^0$
11	Cu	422.793,570.6,666.07	-	-
12	C	193.02,247.88	$2s^2 2P^2\ ^1S$	$2S^2 2P^3 S\ ^1P^0$
13	H	656.28	$2s\ ^2S$	$3p^2 P^0$
14	CN	383.75,383.40,383	-	-

applied 400mJ laser energy and 0.1 mu s delay to obtain LIBS spectra. The visible lines are listed and pointed out in Table 2.

Differentiation and Detection of microbial spectrum

This kind of bacterial tester can be recognized by the features of LIBS spectra as follows:

a. Quantitating relative intensity of C-247, C-193, H and H-alpha.

b. Introduction of intensity of indications of dissimilar elements in various bacteria.

c. Ratio of intensity of various peaks of elements.

Calibration of C 247, C 193 also H alpha comparative intensities

The bacteria tests indicated that there were lines in carbon at 193.02 nm and 247.88 nm and a H line at 656.28 nm. Because most of the biomaterials are C and H, these lines can guide us to detect and paste a lot of similar lines in Table 3, we give the strength values of the C-247, C-193 of each bacterium and H in air. In case of E. coli the green-colored bars for carbon and hydrogen are observed to be conspicuously stronger than those registered in the case of S. aureus and Micrococcus luteus. Moreover, the intensities of Na I Mg I fine, and are higher in E. coli as compared with S. aureus.Also, it is only when bacteria are identified by the presence of carbon and hydrogen bands, in infrared citation that it can be considered with the most certainty [37].

Intensity ratio of various peaks of elements

Line strengths of fashionable LIP, but percentages of the intensities of conforming elements are often equal in specific nature of materials [30,31]. Intensity ratios of dissimilar

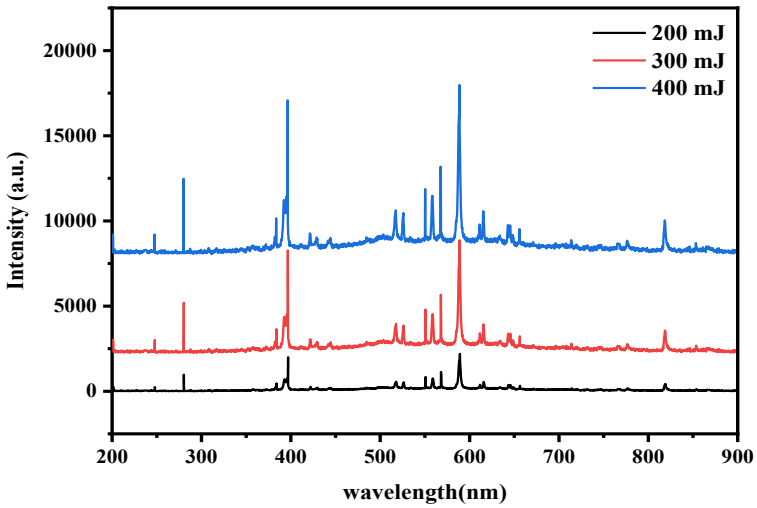

Fig 10. Consequence of laser energy on LIBS amount.

Table 3. Comparative intensity of C and H in *E. coli*, *S. aureus* and *Micrococcus luteus*.

Element	*E. coli*	*S. aureus*	Micrococcus luteus
656.28 nm carbon line	321	679	370
247.88nm Carbon line	250	320	434
589.48 Ca group	2200	2600	997

Table 4. Comparative concentration of carbon and hydrogen in *E. coli*, *S. aureus* and *Micrococcus luteus*.

Element	*E. coli*	*S. aureus*	*Micrococcus luteus*
656.28 nm Carbon line	321	679	370
247.88nm Carbon line	250	320	434
589.48 Ca group	2200	2600	997

elements are observed to the hydrogen line 656 observed in LIP fields. Besides, CN molecular signals are observed in the LIP spectra with bacterial samples.

Laser energy-induced peak intensity during bacteria

The nature of the radiation emitted by laser-plasmas varied with the pulse energy that we had found. The definition of fluency Often physicists will define fluency as the rate of passage of a radiation or particle through a material measured instantaneously. In laser optics, fluency of a pulse is the amount of optical energy that takes strike on unit area. The most common of its units include J/cm^2. Laser energy in the pulse, and the area of the target are the only parameters which influence the energy density of a laser beam on that target. In removing an atom from a surface using a laser pulse, the fluency of the laser must be greater than the binding energy of the material under which its being operated as seen Fig. 10. Effect of laser pulsed on the bacter screen which was peak of concentration bacteria media with rise of laser energy, the intensity augmented in respect to species opacity and mass of the expelled matter.

CONCLUSION

S. aureus and E. coli have been subjected to LIBS techniques in single colony form. The evaluation of the CN band head intensity provides an idea of the extent to which the bonds of natural CN molecules participate in the chemical mixture of the medium. We observed CN bonds in the S. aureus and E. coli on using recorded spectra, and the outcome of the air and native binding of the bacteria CN bonds. According to the experiments, the key step of ablation work at a given laser fluence can be exhibited by the correlation between the dynamics of carbon atomic bonds with covalent bonds of CN. So Nd:YAG Thus, since LIBS combines the understanding of the spectrum of the molecules with information on the spectra of atoms, it can be employed when it comes to organic or biological materials. The difference between the samples on the level of bacteria can also be established by observing dissimilarities in trace elements and the intensity of the carbon and hydrogen lines.

CONFLICT OF INTEREST

The authors declare that there is no conflict of interests regarding the publication of this manuscript.

REFERENCES

1. Harilal SS, O'Shay B, Tillack MS, Mathew MV. Spectroscopic characterization of laser-induced tin plasma. J Appl Phys. 2005;98(1).
2. Cremers DA, Radziemski LJ. Handbook of Laser-Induced Breakdown Spectroscopy: Wiley; 2006 2006/04/21.
3. Anabitarte F, Cobo A, Lopez-Higuera JM. Laser-Induced Breakdown Spectroscopy: Fundamentals, Applications, and Challenges. ISRN Spectroscopy. 2012;2012:1-12.
4. Mohamed A. Mechanical performance of aluminum-silicon casting alloys for high-temperature applications. Qatar Foundation Annual Research Forum Volume 2012 Issue 1: Hamad bin Khalifa University Press (HBKU Press); 2012.
5. Song K, Lee Y-I, Sneddon J. Applications of Laser-Induced Breakdown Spectrometry. Applied Spectroscopy Reviews. 1997;32(3):183-235.
6. Abdellatif G, Imam H. A study of the laser plasma parameters at different laser wavelengths. Spectrochimica Acta Part B: Atomic Spectroscopy. 2002;57(7):1155-1165.
7. Müller K, Stege H. Evaluation of the Analytical Potential of Laser-Induced Breakdown Spectrometry (Libs) for the Analysis of Historical Glasses*. Archaeometry. 2003;45(3):421-433.
8. Alshathr AH, Hatem T, Al-Majeed MA, Saadoon NM, Rahmah MI. Breakdown Spectroscopy Stimulate by Laser for Silver Plasma. Neuroquantology. 2022;20(1):84-89.
9. Gondal M, Hussain T, Yamani Z, Baig M. The role of various binding materials for trace elemental analysis of powder samples using laser-induced breakdown spectroscopy. Talanta. 2007;72(2):642-649.
10. Thakur SN, Singh JP. Fundamentals of Laser Induced Breakdown Spectroscopy. Laser-Induced Breakdown Spectroscopy: Elsevier; 2007. p. 3-21.
11. Russo RE, Mao XL, Yoo J, Gonzalez JJ. Laser ablation. Laser-Induced Breakdown Spectroscopy: Elsevier; 2007. p. 41-70.
12. Portnov A, Rosenwaks S, Bar I. Emission following laser-induced breakdown spectroscopy of organic compounds in ambient air. Appl Opt. 2003;42(15):2835.
13. Cremers DA, Multari RA, Knight AK. Laser-Induced Breakdown Spectroscopy. Encyclopedia of Analytical Chemistry: Wiley; 2016. p. 1-28.
14. Anzano JM, Bello-Gálvez C, Lasheras RJ. Identification of Polymers by Means of LIBS. Springer Series in Optical Sciences: Springer Berlin Heidelberg; 2014. p. 421-438.
15. Liu K, Tian D, Li C, Li Y, Yang G, Ding Y. A review of laser-induced breakdown spectroscopy for plastic analysis. TrAC, Trends Anal Chem. 2019;110:327-334.
16. Negre E, Motto-Ros V, Pelascini F, Yu J. Classification of plastic materials by imaging laser-induced ablation plumes. Spectrochimica Acta Part B: Atomic Spectroscopy. 2016;122:132-141.
17. Mohaidat Q, Palchaudhuri S, Rehse SJ. The Effect of Bacterial Environmental and Metabolic Stresses on a Laser-Induced Breakdown Spectroscopy (LIBS) Based Identification of Escherichia coli and Streptococcus viridans. Applied Spectroscopy. 2011;65(4):386-392.
18. Liang JH, Wang SQ, Zhang WF, Guo Y, Zhang Y, Chen F, et al. Rapid and accurate identification of bacteria utilizing laser-induced breakdown spectroscopy. Biomedical Optics

Express. 2024;15(3):1878.
19. Rehse SJ, Salimnia H, Miziolek AW. Laser-induced breakdown spectroscopy (LIBS): an overview of recent progress and future potential for biomedical applications. Journal of Medical Engineering and Technology. 2012;36(2):77-89.
20. Abdel-Harith M, Abdel-Salam Z. Reflection-enhanced laser-induced fluorescence spectroscopy to improve the analytical sensitivity in liquids. Spectrochimica Acta Part A: Molecular and Biomolecular Spectroscopy. 2023;289:122230.
21. Rodat A, Gavard P, Couderc F. Improving detection in capillary electrophoresis with laser induced fluorescence via a bubble cell capillary and laser power adjustment. Biomed Chromatogr. 2008;23(1):42-47.
22. Abdollahi Jahdi S, Parvin P, Seyedi S, Jelvani S, Razzaghi MR. Spectroscopic Characteristics of Xeloda Chemodrug. Journal of Lasers in Medical Sciences. 2021;12(1):e51-e51.
23. Samek O, LiŠKa M, Kaiser J, Beddows DCS, Telle HH, Kukhlevsky SV. Clinical Application of Laser-Induced Breakdown Spectroscopy to the Analysis of Teeth and Dental Materials. Journal of Clinical Laser Medicine and Surgery. 2000;18(6):281-289.
24. Hybl JD, Lithgow GA, Buckley SG. Laser-Induced Breakdown Spectroscopy Detection and Classification of Biological Aerosols. Applied Spectroscopy. 2003;57(10):1207-1215.
25. Szökő É, Tábi T. Analysis of biological samples by capillary electrophoresis with laser induced fluorescence detection. Journal of Pharmaceutical and Biomedical Analysis. 2010;53(5):1180-1192.
26. Senesi GS, Dell'Aglio M, Gaudiuso R, De Giacomo A, Zaccone C, De Pascale O, et al. Heavy metal concentrations in soils as determined by laser-induced breakdown spectroscopy (LIBS), with special emphasis on chromium. Environ Res. 2009;109(4):413-420.
27. Baudelet M, Guyon L, Yu J, Wolf J-P, Amodeo T, Fréjafon E, et al. Femtosecond time-resolved laser-induced breakdown spectroscopy for detection and identification of bacteria: A comparison to the nanosecond regime. J Appl Phys. 2006;99(8).
28. Delserieys A, Khattak FY, Lewis CLS, Riley D. Optical Thomson scatter from a laser-ablated magnesium plume. J Appl Phys. 2009;106(8).
29. Jovanovic S. Ian Ward: Introduction to critical legal theory, Cavendish Publishing, London, 2004, str. 215. Temida. 2005;8(2):45-46.
30. Kartal B, Geerts W, Jetten MSM. Cultivation, Detection, and Ecophysiology of Anaerobic Ammonium-Oxidizing Bacteria. Methods in Enzymology: Elsevier; 2011. p. 89-108.
31. Jasim MN, Ahmed Kareem S. The Study of Optical and Structural Properties of NiO - SnO2: CdO Nanostructures Thin Films. Iraqi Journal of Nanotechnology. 2022(3):11-19.
32. Abdi A, Hussen S, Ahmed M. Author response for "Prevalence, Antimicrobial Susceptibility Pattern and Associated Factors of Staphylococcus Aureus Among Camel's Raw Milk in Babile District, Oromia, Ethiopia". Wiley; 2025.
33. Rahmah MI, Saadoon NM, Mohasen AJ, Kamel RI, Fayad TA, Ibrahim NM. Double hydrothermal synthesis of iron oxide/silver oxide nanocomposites with antibacterial activity **. Journal of the Mechanical Behavior of Materials. 2021;30(1):207-212.
34. Saadoon NM, Hadi NM, Sabeeh SH. Diagnosis of copper plasma by laser induced breakdown spectroscopy. IOP Conference Series: Materials Science and Engineering. 2020;757(1):012023.
35. Blosi M, Albonetti S, Dondi M, Martelli C, Baldi G. Microwave-assisted polyol synthesis of Cu nanoparticles. J Nanopart Res. 2010;13(1):127-138.
36. Bennett Chandran C, Subramanian TV, Arthur Felse P. Chemometric optimisation of parameters for biocatalytic reduction of copper ion by a crude enzyme lysate of Saccharomyces cerevisiae grown under catabolic repression conditions. Biochem Eng J. 2001;8(1):31-37.
37. Hadi EM, Naji RM, Khalee HL, Saadoon NM, Mohammed MN, Abdullah TA, et al. Study the Sensing Properties of Gold, Silver, and Aluminium Coupling Plasmon Nano-Sphere and Homo-Dimers. Research Square Platform LLC; 2024.